

ORIGINAL ARTICLE

# Observational study of the microcirculation in patients with liver cirrhosis

Stephen Wythe,<sup>\*,†</sup> Thomas W Davies,<sup>\*,†</sup> James O'Beirne,<sup>\*,‡,§</sup> Daniel Martin<sup>\*,†</sup> and Edward Gilbert-Kawai<sup>\*</sup>

<sup>\*</sup>University College London Centre for Altitude Space and Extreme Environment Medicine, UCLH NIHR Biomedical Research Centre, Institute of Sport and Exercise Health, <sup>†</sup>Department of Intensive Care, Royal Free Hospital Pond Street, London, UK, <sup>‡</sup>Department of Hepatology, Sunshine Coast University Hospital, Sunshine Coast Hospital and Health Service, Brisbane and <sup>§</sup>University of the Sunshine Coast, Sunshine Coast Region, Queensland, Australia

## Key words

cirrhosis, hepatology, incident dark field imaging, microcirculation, near infra-red spectroscopy, video microscopy.

Accepted for publication 17 April 2019.

## Correspondence

Stephen Wythe, Homerton University Hospital, Homerton Row, London, E9 6SR, UK.  
Email: s.wythe@nhs.net

**Declaration of conflict of interest:** There are no conflicts of interest to declare, from any of the authors, in relation to this research.

## Abstract

**Background and Aim:** Liver cirrhosis is associated with widespread microcirculatory dysfunction and hemodynamic derangement, which may play a role in the pathogenesis of multiple organ failure. Little is known, however, about the progression of microvascular alterations as the severity of liver disease worsens. Therefore, our aim is to quantify the peripheral systemic microcirculatory changes associated with increasing severity of liver cirrhosis.

**Methods:** Forty patients with liver cirrhosis were studied and divided into groups based on Child-Pugh classes A ( $n = 9$ ), B ( $n = 18$ ), and C ( $n = 13$ ) for comparison. Incident dark field imaging was used to evaluate the sublingual microcirculation and near-infrared spectroscopy at the thenar eminence to assess microvascular reactivity and function.

**Results:** There was no difference in microcirculatory flow index ( $P = 0.655$ ), heterogeneity index ( $P = 0.702$ ), or vessel density ( $P = 0.923$ ) between the different Child-Pugh groups. Microvascular reactivity did not change as the severity of liver disease worsened.

**Conclusions:** This study showed no association between peripheral systemic microcirculatory alterations and the severity of liver disease. Further research with larger study cohorts are needed to clarify the relationship between microcirculatory abnormalities and disease progression and to establish if the peripheral microcirculation is affected by the pathophysiology of worsening cirrhosis.

## Introduction

In developed countries, the rate of liver cirrhosis is rising. It is now the fifth most common cause of death in the United Kingdom and the only major cause that continues to rise.<sup>1,2</sup> As the disease advances, widespread intra- and extrahepatic microvascular alterations occur. Histological changes in the intrahepatic microcirculation include capillarization of sinusoids, angiogenesis, and microvascular venous thrombosis<sup>3</sup>—all of which increase hepatic vascular resistance and lead to portal hypertension.<sup>4–6</sup> The systemic macrocirculatory effects of cirrhosis are also well described. Classically, there is a hyperdynamic, dilated systemic circulation<sup>7</sup> characterized by increased cardiac output and heart rate (HR), with a low systemic vascular resistance.<sup>5</sup> At the same time, there are contrasting findings demonstrated in extrahepatic vascular beds, with reduced blood flow observed in peripheral limbs and renal and cerebral vasculature.<sup>7–13</sup> While the state of extrahepatic microcirculation is more poorly understood, initial studies have demonstrated heterogeneous alterations and microcirculatory dysfunction when compared to controls.<sup>14</sup> The role of these

alterations in the pathogenesis of organ failure with increasing severity of liver cirrhosis, however, remains unclear.

In recent years, evidence has emerged that microcirculatory dysfunction is an important component in the pathophysiology of sepsis.<sup>15</sup> Using video microscopy techniques, direct in vivo observation of the sublingual microcirculation in sepsis has shown an association between the degree of microcirculatory dysfunction present and progression to multiorgan failure.<sup>16–18</sup> Near-infrared spectroscopy (NIRS) is an additional noninvasive tool that has been used to assess microvascular function in sepsis—in this instance through the measurement of tissue oxygen saturation (StO<sub>2</sub>). Studies using NIRS in combination with a vascular occlusion test (VOT) have demonstrated an association between both impaired oxygen delivery and a slower recovery from a hypoxic challenge<sup>19</sup> and an increased mortality rate in patients with sepsis.<sup>20</sup> Similar to sepsis, advanced cirrhosis is a systemic, inflammatory, multiorgan syndrome often associated with hemodynamic derangement, and as such, studying the microcirculation in cirrhosis using these techniques may provide insight into the pathophysiology of multiple organ failure in end-stage liver disease.

In this study, we aimed to quantify peripheral systemic microcirculatory changes associated with the increasing severity of liver cirrhosis using incident dark field (IDF) imaging video microscopy and NIRS-VOT. We tested the hypothesis that a greater Child-Pugh score would be associated with reduced microcirculatory flow and impaired microvascular reactivity.

## Methods

**Study participants.** Ethical approval for the study was obtained from the London Queen Square Research Ethics Committee on behalf of the National Research Ethics Service, and all participants provided written informed consent.

Participants were eligible for inclusion in the study if they had a diagnosis of liver cirrhosis made by a specialist hepatologist (cirrhosis was diagnosed by previous liver biopsy or by compatible clinical, biochemical, or radiological investigations) and were over 18 years of age. Exclusion criteria included dementia, learning difficulties, or pre-existing mental incapacity.

**Study setting.** This study was conducted between June 2016 and August 2017 at the Royal Free Hospital in London, a university teaching hospital with a tertiary specialist liver unit. Patients were identified and recruited from the hepatology ward, intensive care unit, and the planned investigation and treatment unit (PITU).

**Physiological measurements and grading of severity of liver disease.** All patients underwent a complete physical examination. Peripheral oxygen saturation (SpO<sub>2</sub>), HR, blood pressure (BP), and tympanic temperature were measured. The presence of ascites and encephalopathy was recorded. Clinical evaluation guided the severity of ascites, and encephalopathy was graded using the West-Haven criteria. The severity of cirrhosis was classified by the Child-Pugh Score, and patients were subsequently divided into three groups—Child-Pugh classes A, B, and C. Blood tests were taken routinely as part of the participants' ongoing clinical care, and no additional blood tests were required as part of the study.

**Observation of the sublingual microcirculation.** The microcirculation of each participant was visualized using the Braedius Cytocam Incident Dark Field video microscope (Braedius Medical, Huizen, the Netherlands)<sup>21</sup>. Participants were required to rest for 5 minutes prior to the investigation. The IDF camera probe was then positioned beneath the participant's tongue, and the camera was focused to obtain images following the standard operating guidelines of Trzeciak *et al.*<sup>22</sup> Twenty seconds of video footage were digitally recorded onto the computer, and the process was then repeated to acquire three good-quality recordings from different regions underneath the tongue of each participant. All images were obtained by one of two investigators, both of whom had extensive experience using the Cytocam.

**Analysis of microcirculatory video images.** Blinded IDF data analysis was conducted by two trained investigators using the Automated Vascular Analysis (AVA) 3.2 microcirculatory analysis software (MicroVision Medical, Amsterdam, the Netherlands).<sup>23</sup> Videos were only considered acceptable for

analysis if they adhered to the "microcirculation image quality score."<sup>24</sup> Using the analysis software, image contrast was optimized, and all videos underwent image stabilization. Following initial automatic recognition of blood vessels, undetected vessels were redrawn manually, and any errors were corrected. The IDF variables measured were microvascular flow index (MFI),<sup>25,26</sup> heterogeneity index (HI), and small vessel density (see Appendix for further description of the IDF measures).

**Measurement of muscle oxygen saturation.** Thenar muscle oxygenation was measured by NIRS in combination with a VOT. The InSpectra™ Tissue Spectrometer (Model 325; Hutchinson Technology Inc., Hutchinson, MN, USA) was used, incorporating a 15 mm probe. StO<sub>2</sub> was calculated from the ratio of oxygenated to total hemoglobin in the NIRS signal reflected from tissue below the probe.

The NIRS probe was placed on the thenar eminence of the passively supinated dominant hand and taped around its edges to reduce any effect that excessive ambient light might produce. The VOT was performed using a BP cuff placed around the upper limb proximal to the NIRS probe. Participants rested for a minimum of 10 min in the semirecumbent position, with their arms straight on the bed at the level of the heart, prior to the commencement of recordings. After a 3-min period of stabilization with baseline StO<sub>2</sub> recordings, the VOT protocol was commenced. The BP cuff was rapidly inflated (3–4 s) to 250 mmHg for 3 min and then deflated. NIRS data collection continued for 5 min following cuff release. The exact times of occlusion and deflation were electronically marked on the NIRS tracing. The electronic data were analyzed using the automated "InSpectra StO<sub>2</sub> Researcher's Analysis Software" (Hutchinson Technology, MN, USA). The following variables were derived: baseline, minimum and peak StO<sub>2</sub> (%); StO<sub>2</sub> down slope (% per minute) and StO<sub>2</sub> up slope (% per second); area under the recovery curve (%/min); and the recovery time (s) (see Appendix for further description of NIRS measures).

**Analysis and statistical technique.** Data were first tested for Gaussian distribution using the Kolmogorov–Smirnov test and visual inspection of histograms. As the data did not show normal distribution, all data are presented as median (interquartile range). Data from the three Child-Pugh class groups were compared using the Kruskal–Wallis with Bonferroni correction for pairwise comparison. To further investigate if other variables had any effect on the microcirculation, we divided the data into a control group and comparison group depending on:

1. Model for End-Stage Liver Disease (MELD)<sup>27</sup> score > 10
2. Active infection (on antibiotic treatment at time of study)
3. Renal dysfunction (creatinine level of >100 μmol/L)
4. Presence of moderate or severe ascites
5. Presence of encephalopathy.

These subgroups were compared using the Mann–Whitney *U* test. Calculations were performed using SPSS version 23.0 (IBM Corp., Armonk, NY, USA), and a *P* value of <0.05 was considered to indicate statistical significance.

**Table 1** Demographic characteristics of study participants

	Child-Pugh class		
	A	B	C
Number	9	18	13
Gender (% male)	55	66	54
Age (years)	64.7 ( $\pm 7.7$ )	59.9 ( $\pm 11.4$ )	49.1 ( $\pm 12.3$ )
Height (cm)	172.3 ( $\pm 8.8$ )	172.4 ( $\pm 10.2$ )	169.3 ( $\pm 8.9$ )
Weight (kg)	78.5 ( $\pm 13.6$ )	88.4 ( $\pm 27.5$ )	80.8 ( $\pm 24.4$ )
Etiology (% ALD)	44	28	62

Data are expressed as mean value (standard deviation).  
ALD, alcoholic liver disease.

## Results

Data were collected for 40 patients of Child-Pugh classes A ( $n = 9$ ), B, ( $n = 18$ ) and C ( $n = 13$ ). Demographic and biochemical data can be found in Tables 1 and 2, respectively.

**Table 2** Biochemical tests and MELD score

	Child-Pugh class			<i>P</i> value
	A	B	C	
Bilirubin (mmol/L)	19 (17–24)	26 (19–37)	129 (90–211)	<0.001
Albumin (g/dL)	37 (33–38)	32 (30–33)	30 (25–33)	0.005
INR	1.3 (1.2–1.4)	1.4 (1.3–1.5)	1.9 (1.7–2.3)	<0.001
Urea (mmol/L)	8.2 (6.3–9.2)	9.2 (6.1–12.2)	6.0 (4.5–8.9)	0.461
Creatinine (mmol/L)	86 (79–111)	103 (73–128)	71 (66–92)	0.631
Sodium (mmol/L)	136 (134–140)	138 (134–141)	135 (133–136)	0.174
MELD	12 (10–14)	14 (13–18)	24 (20–26)	<0.001

Data are expressed as median value (interquartile range).  
INR, international normalised ratio; MELD, Model for End-Stage Liver Disease score.

**Table 3** Values for microcirculatory assessment by IDF imaging

	Child-Pugh class			<i>P</i> value
	A	B	C	
Small vessel density (mm/mm <sup>2</sup> )	15.6 (14.0–18.6)	16.3 (14.1–17.2)	16.2 (13.8–17.7)	0.966
Microvascular flow index	2.75 (2.67–2.92)	2.83 (2.42–3.00)	2.75 (2.33–3.00)	0.819
Heterogeneity index	0.36 (0.35–0.38)	0.35 (0.00–0.80)	0.36 (0.00–0.85)	0.859

Data are expressed as median value (interquartile range).

**Table 4** Tissue oxygenation values during vascular occlusion test

	Child-Pugh class			<i>P</i> value
	A	B	C	
Baseline StO <sub>2</sub> (%)	81 (77–84)	81 (74–85)	84 (79–85)	0.722
Minimum StO <sub>2</sub> (%)	49 (42–54)	49 (40–55)	49 (38–53)	0.944
Peak StO <sub>2</sub> (%)	95 (94–98)	94 (90–94)	95 (93–96)	0.247
Occlusion downslope (%/min)	10.7 (9.8–11.5)	10.6 (9.6–11.8)	11.15 (10.8–12.7)	0.454
Recovery upslope (%/s)	4.9 (3.6–5.1)	4.0 (3.0–4.8)	4.4 (3.5–5.1)	0.523
Area under recovery curve (%/minute)	18.2 (10.1–22.9)	14.4 (11.0–20.1)	14.4 (11.8–17.0)	0.652
Recovery time (s)	180 (176–180)	180 (150–180)	180 (156–180)	0.779

Data are expressed as median value (interquartile range).

The IDF microcirculatory data are presented in Table 3, and NIRS data are presented in Table 4. There were no statistically significant differences in any of the IDF microcirculatory parameters (small-vessel MFI, HI, and density—see Figs 1–2, and 3, respectively) between the different Child-Pugh groups or in any of the NIRS-VOT data.

The subgroup analysis data are presented in Table 5. There were no significant differences in microcirculatory flow or function between patients with MELD score >10 ( $n = 21$ ), active infection ( $n = 14$ ), renal dysfunction ( $n = 17$ ), moderate to severe ascites ( $n = 15$ ), or encephalopathy ( $n = 14$ ) when each of these groups was compared to the remainder of the study cohort (control group).

## Discussion

This is the first study to use combined IDF imaging and NIRS-VOT to examine the effects of increasing severity of liver cirrhosis on the peripheral systemic microcirculation. Our findings

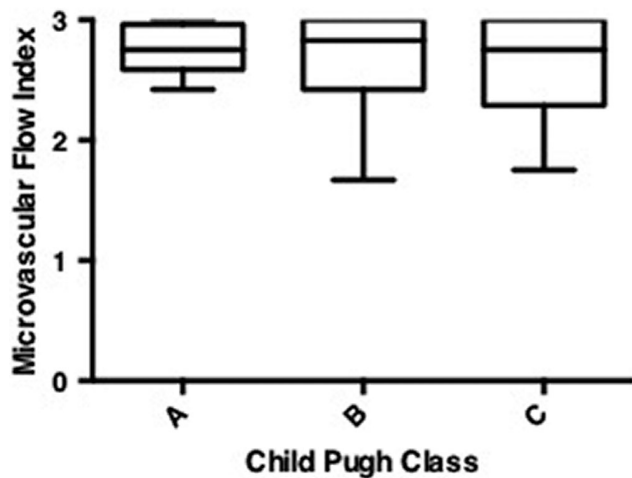


**Figure 1** Boxplot comparing small-vessel (<25  $\mu\text{m}$ ) microvascular flow index between Child-Pugh classes A, B, and C patients.

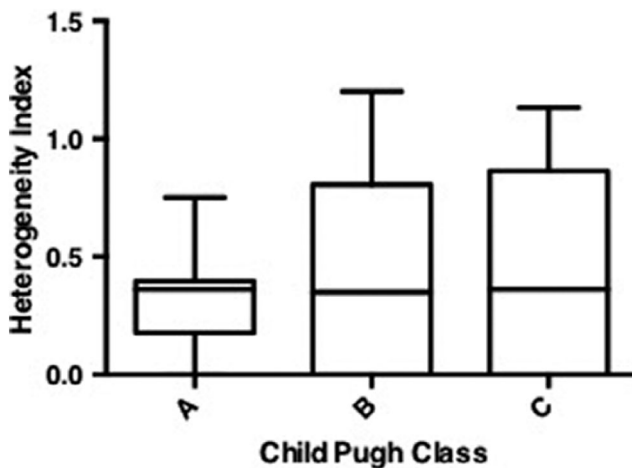


**Figure 2** Boxplot comparing small-vessel (<25  $\mu\text{m}$ ) heterogeneity index between Child-Pugh classes A, B, and C patients.

show that there was no difference in microcirculatory flow or reactivity as the severity of liver cirrhosis worsened.

This contradicts previous work by Sheikh *et al.*,<sup>28</sup> who demonstrated significant differences in sublingual small-vessel MFI between groups of compensated and decompensated cirrhotics (MFI scores of  $2.40 (\pm 0.46)$  vs  $1.40 (\pm 0.52)$ , respectively), inferring a reduction in microvascular flow as cirrhosis decompensates. Our data are more consistent with a recent study<sup>14</sup> using SDF (Sidestream Dark Field) imaging to compare the microcirculation of patients with cirrhosis and healthy controls; the authors reported a much smaller difference between healthy controls (MFI scores  $3.0 \pm 0.0$ ) and those with cirrhosis (MFI scores  $2.9 \pm 0.1$ ) but found that, in the cirrhosis group, there was no difference in MFI values according to Child-Pugh or MELD scores. Finally, Reynolds *et al.*<sup>29</sup> found no significant differences when comparing the sublingual microcirculation of patients with cirrhosis and a healthy control group.

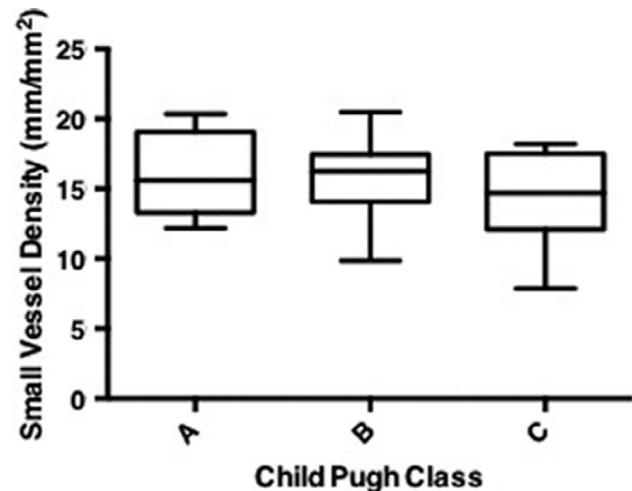


**Figure 3** Boxplot comparing small-vessel (<25  $\mu\text{m}$ ) density in Child-Pugh classes A, B, and C patients.

Clearly, these results are contradictory, and when placed alongside our nonsignificant findings, it is difficult to draw conclusions. This may, however, partly relate to the fact that significant disparities exist between the different study populations and design. Sheikh *et al.*<sup>28</sup> studied a population of mainly Child-Pugh B and C patients (31/45), whereas Reynolds *et al.*<sup>29</sup> study focused almost entirely on Child-Pugh A patients (17/18). It has been well described that, during the progression of cirrhosis, there is marked systemic and splanchnic vasodilation in order to maintain portal flow in the face of increased vascular resistance in the liver.<sup>30</sup> This occurs at the expense of other organs, eventually leading to the activation of vasoconstrictor mechanisms later in the pathophysiological process.<sup>31</sup> Therefore, perhaps the disparity in the severity of disease between study groups has led to measurements taken in the early “vasodilatory phase” (Reynolds *et al.*,<sup>29</sup> increased MFI) and later “vasoconstrictive phase” (Sheikh *et al.*,<sup>28</sup> decreased MFI). Nevertheless, our study tested patients with cirrhosis of variable severity and failed to show any difference with increasing burden of liver disease.

Gonzalez Ballerga *et al.*<sup>14</sup> were able to demonstrate some small but significant differences between the systemic microcirculation of cirrhotic patients when compared with a group of healthy controls in contrast to Reynolds *et al.*<sup>29</sup> Importantly, their control group was matched for age, gender, and cardiovascular risk factors, all of which may have allowed for greater accuracy and clearer indication of the changes attributable to cirrhosis. The most marked finding in their study was an increase in heterogeneity index (0.36 vs 0.64), which has also been described in the microcirculation during sepsis,<sup>32,33</sup> alongside other changes of decreased vessel density and reduced flow.<sup>16</sup> It is possible therefore that, due to inadequate powering of our study and/or because we compared different groups of varying severity of cirrhosis to each other rather than against controls, any microcirculatory differences that may exist were not detected. Unfortunately, Sheikh *et al.*<sup>28</sup> and Reynolds *et al.*<sup>29</sup> did not publish HI data, so a comparison with their studies is not possible.

Our NIRS data also did not show any differences in microcirculatory function with worsening liver disease. A

**Table 5** Sub group analysis

	Subgroup analyses ( <i>P</i> value)				
	MELD > 10 ( <i>n</i> = 21)	Active Infection ( <i>n</i> = 14)	Renal dysfunction ( <i>n</i> = 17)	Ascites ( <i>n</i> = 15)	Encephalopathy ( <i>n</i> = 14)
Small vessel density (mm/mm <sup>2</sup> )	0.872	0.254	0.644	0.581	0.922
Microvascular flow index	0.469	0.856	0.362	0.562	0.457
Heterogeneity index	0.452	0.726	0.232	0.439	0.685
Baseline StO <sub>2</sub> (%)	0.573	0.922	0.292	1.000	0.408
Minimum StO <sub>2</sub> (%)	0.520	0.812	0.027†	0.489	0.856
Peak StO <sub>2</sub> (%)	0.936	0.231	0.624	0.192	0.547
Occlusion downslope (%/min)	0.592	0.944	0.059	0.659	0.834
Recovery upslope (%/s)	0.768	0.624	0.077	0.078	0.332
Area under recovery curve (%/minute)	0.469	0.812	0.059	0.525	0.685
Recovery time (s)	0.452	0.726	0.726	0.581	0.834

Data are expressed as *p* value by Mann-Whitney U test. Control group is remainder of study cohort (=40-*n*). MELD = Model for End Stage Liver Disease. † = Significant difference demonstrated between sub group and control group (*p* < 0.05).

previous study used NIRS in liver cirrhosis,<sup>34</sup> demonstrating a vasodilatory state, with the variables suggesting hyperemia (area under recovery curve, recovery time) increased compared to healthy controls, although no difference was seen in StO<sub>2</sub> up- or downslope. The authors were also able to show, through subgroup analyses, that the hyperemia was more marked for worsening Child-Pugh scores. The study population included outpatients with cirrhosis and included a larger proportion of Child-Pugh A (11/25) patients than B or C; as such, none were acutely decompensated or unwell. It has already been suggested, in the context of our IDF data, that perhaps earlier stages of the disease have a tendency to vasodilation, and later stages (or decompensation) may trigger activation of vasoconstrictor systems. The disparity with regard to our results could be another reflection of this phenomenon.

**Strengths and limitations.** This study used robust methods and well-validated techniques to study the microcirculation. The Cytocam video microscope has demonstrated superior capabilities in image acquisition compared to its predecessor SDF imaging, which was used in previous studies examining the sublingual microcirculation in cirrhosis.<sup>35</sup> To date, there have been few studies, all with small sample sizes, examining the peripheral microcirculation in cirrhosis and our findings add to the current body of knowledge on this topic.

There are also a number of limitations to our study. The first thing to consider is the context in which our participants were recruited. The higher Child-Pugh scores were seen in patients with acute on chronic liver failure (ACLF) and also in patients with compensated advanced cirrhosis who were attending routine outpatient appointments for ascitic drains or transplant workup. Despite a similar Child-Pugh score, the ACLF patients may actually have had more microcirculatory dysfunction, thus skewing the observed results for the Child-Pugh B and C groups, reducing the observable differences. Furthermore, many of the critically ill patients we saw in intensive care were treated with vasopressors and inotropes to optimize their circulation, which may have reduced the observed severity of microcirculatory dysfunction in the Child Pugh C group even further. Second, each group contained a

mixture of etiologies (both of the underlying disease causing cirrhosis and of the cause of decompensation), and this may have contributed to the heterogeneity within patient groups. In light of this, we did undertake subgroup analyses comparing patients with MELD score >10, active infection, renal dysfunction, encephalopathy, and ascites with the rest of the cohort, but the data did not demonstrate any differences. That said, given that our methods were not designed to study those specific questions, the results generated should be interpreted with caution. Unfortunately, we did not measure the CLIF-C ACLF score, which may have been useful to further compare patients. Another limitation to this study is sample size—although ours is not dissimilar to other studies in this area. Nonetheless, this certainly contributes to difficulty detecting differences between groups and adds to heterogeneity within the data as matching groups for variables other than severity of liver cirrhosis is a significant challenge.

The peripheral systemic microcirculation in cirrhosis has still not been well characterized. Given the dissimilar, and at times contradictory, findings detailed above, it is difficult to draw outright conclusions from our data about the state of the peripheral systemic microcirculation in cirrhosis. Evidence of heterogeneous microvascular alterations exists, but the association with severity of disease and clinical outcome remains unknown. This uncertainty leaves unanswered questions and further work to be carried out. Larger studies with appropriate study populations and adequate sample sizes are required to accurately describe the microcirculation and determine the exact nature of these potential alterations. Direct monitoring of the microcirculation in vivo, potentially with the advent of automated IDF image analysis, could not only aid us to better understand the heterogeneous nature of the microcirculation in cirrhosis but also enable us to quantify the effects of therapeutic interventions upon it and evaluate the relationship with progression of liver disease and organ failure.

In conclusion, this study showed no association between the peripheral systemic microcirculatory alterations and severity of liver cirrhosis. The role of the extrahepatic microcirculation in the pathophysiology of advanced cirrhosis remains to be determined, and further research with larger study cohorts is needed

to clarify the relationship between microcirculatory abnormalities and progression of chronic liver disease.

## Acknowledgment

We thank the Department of Intensive Care at the Royal Free Hospital London, particularly the Research Office.

## References

- Williams R, Alexander G, Armstrong I *et al.* Disease burden and costs from excess alcohol consumption, obesity, and viral hepatitis: fourth report of the Lancet Standing Commission on Liver Disease in the UK. *Lancet*. 2017; **391**: 1097–107.
- Ge PS, Runyon BA. Treatment of patients with cirrhosis. *N. Engl. J. Med.* 2016; **375**: 767–77.
- Bosch J. Vascular deterioration in cirrhosis: the big picture. *J. Clin. Gastroenterol.* 2007; **41**: 247–53.
- Chen ML, Zeng QY, Huo JW, Yin XM, Li BP, Liu JX. Assessment of the hepatic microvascular changes in liver cirrhosis by perfusion computed tomography. *World J. Gastroenterol.* 2009; **15**: 3532–7.
- Iwakiri Y, Groszmann RJ. The hyperdynamic circulation of chronic liver diseases: from the patient to the molecule. *Hepatology*. 2006; **43**: 121–31.
- Groszmann RJ, Abraldes JG. Portal hypertension: from bedside to bench. *J. Clin. Gastroenterol.* 2005; **39**: 125–30.
- Durand F, Graupera I, Ginès P, Olson JC, Nadim MK. Pathogenesis of hepatorenal syndrome: implications for therapy. *Am. J. Kidney Dis.* 2016; **67**: 318–28.
- Piscaglia F, Zironi G, Gaiani S *et al.* Relationship between splanchnic, peripheral and cardiac haemodynamics in liver cirrhosis of different degrees of severity. *Eur. J. Gastroenterol. Hepatol.* 1997; **9**: 799–804.
- Maroto A, Ginès P, Arroyo V *et al.* Brachial and femoral artery blood flow in cirrhosis: relationship to kidney dysfunction. *Hepatology*. 1993; **17**: 788–93.
- Sacerdoti D, Bolognesi M, Merkel C, Angeli P, Gatta A. Renal vasoconstriction in cirrhosis evaluated by duplex Doppler ultrasonography. *Hepatology*. 1993; **17**: 219–24.
- Rivolta R, Maggi A, Cazzaniga M *et al.* Reduction of renal cortical blood flow assessed by Doppler in cirrhotic patients with refractory ascites. *Hepatology*. 1998; **28**: 1235–40.
- Guevara M, Bru C, Ginès P *et al.* Increased cerebrovascular resistance in cirrhotic patients with ascites. *Hepatology*. 1998; **28**: 39–44.
- Sugano S, Yamamoto K, Atobe T *et al.* Postprandial middle cerebral arterial vasoconstriction in cirrhotic patients. A placebo, controlled evaluation. *J. Hepatol.* 2001; **34**: 373–7.
- Gonzalez Ballerga E, Pozo MO, Rubatto Birri PN *et al.* Sublingual microcirculatory alterations in cirrhotic patients. *Microcirculation*. 2018; **5**: e12448.
- Ince C. The microcirculation is the motor of sepsis. *Crit. Care*. 2005; **9**: 1–7.
- De Backer D, Creteur J, Preiser JC, Dubois MJ, Vincent JL. Microvascular blood flow is altered in patients with sepsis. *Am. J. Respir. Crit. Care Med.* 2002; **166**: 98–104.
- Sakr Y, Dubois MJ, De Backer D, Creteur J, Vincent JL. Persistent microcirculatory alterations are associated with organ failure and death in patients with septic shock. *Crit. Care Med.* 2004; **32**: 1825–31.
- Trzeciak S, JV MC, Phillip Dellinger R *et al.* Early increases in microcirculatory perfusion during protocol-directed resuscitation are associated with reduced multi-organ failure at 24h in patients with sepsis. *Intensive Care Med.* 2008; **34**: 2210–17.
- Neto AS, Pereira VG, Manetta JA, Espósito DC, Schultz MJ. Association between static and dynamic thenar near-infrared spectroscopy and mortality in patients with sepsis: a systematic review and meta-analysis. *J. Trauma Acute Care Surg.* 2014; **76**: 226–33.
- The Emergency Medicine Shock Research Network (EMShockNet). The association of near-infrared spectroscopy-derived tissue oxygenation measurements with sepsis syndromes, organ dysfunction and mortality in emergency department patients with sepsis. *Crit. Care*. 2011; **15**: R223.
- Aykut G, Ince Y, Ince CA. New generation computer-controlled imaging sensor-based hand-held microscope for quantifying bedside microcirculatory alterations. In: *Annual Update in Intensive Care and Emergency Medicine 2014*. Springer International Publishing, New York City, NY, USA, 2014; 367–81.
- Trzeciak S, Dellinger RP, Parrillo JE *et al.* Early microcirculatory perfusion derangements in patients with severe sepsis and septic shock: relationship to hemodynamics, oxygen transport, and survival. *Ann. Emerg. Med.* 2007; **49**: 88–98.
- Dobbe JG, Streekstra GJ, Atasever B, van Zijderveld R, Ince C. Measurement of functional microcirculatory geometry and velocity distributions using automated image analysis. *Med. Biol. Eng. Comput.* 2008; **46**: 659–70.
- Massey MJ, Larochelle E, Najarro G *et al.* The microcirculation image quality score: development and preliminary evaluation of a proposed approach to grading quality of image acquisition for bedside videomicroscopy. *J. Crit. Care*. 2013; **28**: 913–17.
- Boerma EC, Mathura KR, van der Voort PH, Spronk PE, Ince C. Quantifying bedside-derived imaging of microcirculatory abnormalities in septic patients: a prospective validation study. *Crit. Care*. 2005; **9**: 601–6.
- Dubin A, Pozo MO, Ferrara G *et al.* Systemic and microcirculatory responses to progressive hemorrhage. *Intensive Care Med.* 2009; **35**: 556–64.
- Kamath PS, Wiesner RH, Malinchoc M *et al.* A model to predict survival in patients with endstage liver disease. *Hepatology*. 2001; **33**: 464–70.
- Sheikh MY, Javed U, Singh J *et al.* Bedside sublingual video imaging of microcirculation in assessing bacterial infection in cirrhosis. *Dig. Dis. Sci.* 2009; **54**: 2706–11.
- Reynolds T, Jhanji S, Vivian-Smith A, Pearse RM. Observational study of the effects of age, diabetes mellitus, cirrhosis and chronic kidney disease on sublingual microvascular flow. *Peripher. Med.* 2013; **2**: 1–5.
- Schrier RW, Arroyo V, Bernardi M, Epstein M, Henriksen JH, Rodés J. Peripheral arterial vasodilation hypothesis: a proposal for the initiation of renal sodium and water retention in cirrhosis. *Hepatology*. 1988; **8**: 1151–7.
- Newby DE, Hayes PC. Hyperdynamic circulation in liver cirrhosis: not peripheral vasodilatation but “splanchnic steal”. *QJM.* 2002; **95**: 827–30.
- De Backer D, Orbeago Cortes D, Donadello K, Vincent JL. Pathophysiology of microcirculatory dysfunction and the pathogenesis of septic shock. *Virulence*. 2014; **5**: 73–9.
- Edul VS, Enrico C, Laviolle B, Vazquez AR, Ince C, Dubin A. Quantitative assessment of the microcirculation in healthy volunteers and in patients with septic shock. *Crit. Care Med.* 2012; **40**: 1443–8.
- Thomson SJ, Cowan ML, Forton DM *et al.* A study of muscle tissue oxygenation and peripheral microcirculatory dysfunction in cirrhosis using near infrared spectroscopy. *Liver Int.* 2010; **30**: 463–71.
- Gilbert-Kawai E, Coppel J, Bountziouka V, Ince C, Martin D. A comparison of the quality of image acquisition between the incident dark field and sidestream dark field video-microscopes. *BMC Med. Imaging*. 2016; **16**: 10.

## APPENDIX I

### IDF video microscopy measures

1. MFI is a semiquantitative score of microvascular perfusion.<sup>25,26</sup> Quantified on an ordinal scale by a trained observer: 0 = no flow, 1 = intermittent flow, 2 = sluggish flow, 3 = continuous flow. The mean value of the MFIs in each individual vessel was calculated.<sup>26</sup>
2. HI is calculated as the highest site MFI minus the lowest site MFI divided by the mean flow velocity of all sublingual sites at a single time point.<sup>22</sup>
3. Small vessel density (SVD; <25  $\mu\text{m}$  diameter) was calculated by the AVA 3.2 software as relative lengths within the overall field of view ( $\text{mm}/\text{mm}^2$ ).

### NIRS-VOT measures

1. The *downslope* measurement commences at the point where  $\text{StO}_2$  is 0.98 times the baseline  $\text{StO}_2$  and the end-point 1 min later.
2. The start point for *upslope* is determined when the recovery  $\text{StO}_2$  first exceeds 1.05 times the minimum  $\text{StO}_2$  reading and the end-point is when the recovery  $\text{StO}_2$  reaches 0.85 times the baseline  $\text{StO}_2$ .
3. The *area under the recovery curve* is determined by the software and is the integration of the curve above the baseline  $\text{StO}_2$ .
4. The *recovery time* measurement starts when the recovery  $\text{StO}_2$  first exceeds 1.05 times the minimum  $\text{StO}_2$  and ends once it has settled to baseline.